Journal of Chromatography A, 1216 (2009) 933–940

Contents lists available at ScienceDirect

Journal of Chromatography A

journal homepage: www.elsevier.com/locate/chroma

Peptide pore accessibility in reversed-phase chromatography

David Gétaz, Guido Ströhlein, Massimo Morbidelli*

Department of Chemistry and Applied Bioscience, Institute for Chemical and Bioengineering, ETH Zurich, CH-8093 Zurich, Switzerland

ARTICLE INFO

Article history:
Received 19 August 2008
Received in revised form 3 December 2008
Accepted 5 December 2008
Available online 11 December 2008

Keywords:
Reversed-phase
Porosity
Peptide
Pore exclusion
Pore accessibility
Acetonitrile
Adsorption isotherm

ABSTRACT

The effect of salt or peptide concentration on peptide porosity (i.e. the porosity accessible to a given peptide) is investigated on six different reversed-phase stationary phases. The peptide porosity is found to increase with the local concentration of negative charges following a saturation-type function within the same porosity boundaries for both cases. This can induce the formation of anti-Langmuirian peaks in non-adsorbing conditions since the local increase of the ionic strength due to the peptide concentration increases the porosity accessible to the peptide. This behavior can be well reproduced by the ideal model of chromatography assuming non-constant porosity. The acetonitrile adsorption isotherm was also measured on all the considered reversed-phase stationary phases. A comparison between the stationary phases shows a correlation between the amount of acetonitrile accumulated in the pores and the reduced pore accessibility for the peptide.

1. Introduction

Biopharmaceuticals such as peptides and proteins are of growing interest because of their huge potential and efficiency to treat diseases. As chromatography is the most used technique for biomolecule purification, its understanding is of major interest. For this purpose, a fundamental comprehension of chromatographic systems has to be gained. Among the chromatographic techniques, reversed-phase high-performance liquid chromatography (RP-HPLC) is the method of choice for peptide purification. The stationary phase used in RP-HPLC is hydrophobic and consists usually in either highly cross-linked polystyrene or silica particles with bonded alkyl chains. Silica based stationary phases are the most commonly used reversed-phase column and are characterized by narrow pore size distribution and relatively low chemical stability (stable up to pH 8). On the other hand, highly cross-linked polystyrene exhibit broader pore size distribution and higher chemical stability (stable up to pH 12). They are often used for high pH separation and for peptide purification requiring extreme cleaning procedures due to irreversible adsorption [1–5]. Typical modifiers employed in RP-HPLC are non-polar organic compounds such as acetonitrile, tetrahydrofuran or methanol.

The mobile phase volume in a RP-HPLC column, also referred to as the column void volume, is an important parameter. It is used in all calculations and an efficient determination of this volume is essential to improve the prediction accuracy of the chromatographic models. The complexity of the void volume determination comes from the fact that it depends on many parameters such as the eluent composition and the measurement method used [6–14].

The peptide porosity is usually measured at high modifier concentration. In those conditions, the peptide does not adsorb and its retention volume is equivalent to the volume of liquid accessible to the peptide (Fig. 1) [15]. It is observed that in those conditions (i.e. non-adsorbing conditions), peptides can be totally excluded from the pores. However, the high loading capacity observed in adsorbing conditions is only explainable by adsorption of the peptide in the pores. This indicates that the peptide porosity determined in non-adsorbing conditions is not the one experienced by the peptide in adsorbing conditions. Two distinct phenomena affect the peptide pore accessibility and can explain these experimental findings. The first one is an electrostatic effect and the second one is the accumulation of modifier in the pores (i.e. multi-layer adsorption of modifier).

The relevance of the ionic strength in RP-HPLC processes has been highlighted by many authors [16–23,19,23]. Its effect on the adsorption behavior of charged analytes has been extensively studied [20–22,19,23], however, the effect on charged molecules in non-adsorbing conditions has been hardly investigated [16–18]. Neddermeyer and Rogers [24] and Buytenhuys and Van Der Maeden [18] have shown the existence of a Donnan equilibrium resulting from a difference in pore accessibility of two or more salts in gel

* Corresponding author. Tel.: +41 44 6323034; fax: +41 44 6321082.
E-mail address: Morbidelli@chem.ethz.ch (M. Morbidelli).

0021-9673/$ – see front matter © 2008 Elsevier B.V. All rights reserved.
doi:10.1016/j.chroma.2008.12.019

Nomenclature

a	initial slope of the porosity variation (L/mol)
c	analyte concentration in the mobile phase (mol/L)
c_{AcN}	% acetonitrile (v/v)
c_{charge}	negative charge concentration (mol/L)
c_{max}	concentration of pure modifier = 100%
dz	length of the slice (m)
L	length of the column (m)
q	analyte concentration in the solid phase (mol/L)
q_{AcN}	acetonitrile concentration in the solid phase (mol/L)
$q_{AcN,solid}$	acetonitrile concentration in the solid phase (mol/L)
S	solid phase surface (m^2)
t	time (s) or (min)
t_R	retention time (s) or (min)
u_{sf}	superficial velocity (m/s)
V_0	total liquid volume (m^3) or (mL)
V_a	adsorbed phase volume (m^3) or (mL)
$V_{AcN/pore}$	Percentage of pore volume filled with acetonitrile (%)
V_C	column volume (m^3) or (mL)
V_e	interstitial liquid volume (m^3) or (mL)
V_{pore}	pore volume (m^3) or (mL)
V_R	retention volume (m^3) or (mL)
V_S	solid phase volume (m^3) or (mL)
x	non-dimensional length of the column (–)
z	axial coordinate (m)

Greek letters

ε^*	total peptide porosity (–)
ε_e	external porosity (–)
ε^*_{max}	maximal peptide porosity (–)
ε^*_{min}	minimal peptide porosity (–)
ε_p	peptide particle porosity (–)
τ	thickness of the acetonitrile adsorbed layer (m) or (Å)
τ_R	non-dimensional retention time (–)
Γ	excess adsorption isotherm ($\mu mol/m^2$)
Γ_{solid}	excess adsorption isotherm (mol/L)

permeation chromatography. This phenomenon was used by Tsyurupa and Davankov [25] for the development of a new exclusion chromatographic process. Pore exclusion of positively charged analytes and formation of anti-Langmuirian peaks (i.e. peaks having a dispersed front and a compressed (shock) rear) in non-adsorbing conditions has been addressed by several authors [16,18,17]. It has been attributed to electrostatic repulsion between the analyte and the stationary phase by Berendsen et al. [16], presumably due to charged groups on the stationary phase. Loeser [26] has evaluated the surface charge of C18 stationary phases by measuring the flow induced streaming potential and he has concluded that most of the C18 stationary phases have a positive net charge in acidic conditions. The presence of those positive charges remains, however, not clear. It might be due to preferential adsorption of cations relative to anions [27] or to residues of the base used in the bonding process [28]. McCalley [29] has suggested the presence of positively charged group on the surface of commonly used reversed-phase stationary phase. He has shown that ion-exclusion effect induced by those positive charges can be reduced by increasing the pore size and that it leads thus to an increase of protonated bases retention. Loeser and Drumm [30] have also considered the effect of positively charged surface on the retention of basic analyte. He has shown that the pore accessibility increases upon increase of the buffer strength and has considered that ion exclusion may play a significant role in the retention behavior of positively charged analyte, in addition to ion-pairing and chaotropic effects. Several authors have reported a multi-layer adsorption of modifier on usual reversed-phase stationary phase [31–33]. Chan et al. [33] have observed an accumulation of modifier in the pores representing over 60% of the total available pore volume. Kazakevich et al. [31] have developed a retention model assuming the partitioning of the analyte between the mobile phase and the modifier adsorbed phase, followed by its adsorption on the stationary phase surface. This model has been applied to different alkylbenzenes. The effect of the multilayer adsorption of modifier on porosity has been, however, hardly studied. Trathnigg et al. [6] have observed a variation of the pore volume with the mobile phase composition but no explanations were found.

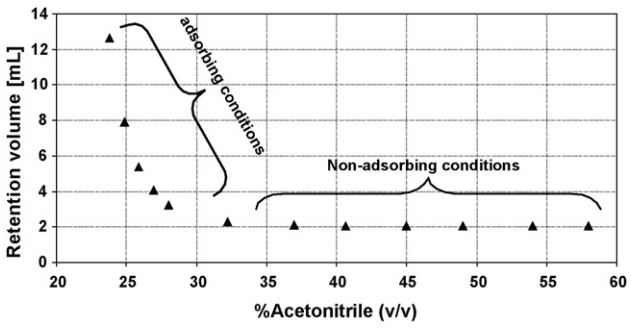

Fig. 1. Peptide retention volume on the RPC column as a function of the acetonitrile content. Mobile phase containing 20 mM Phosphoric acid. Note that above 30–35% AcN, the peptide retention volume is constant and equals to the liquid phase volume accessible to the peptide.

In this work a mathematical model of the porosity variation (i.e. variation of the porosity accessible to a given peptide) as a function of the peptide concentration has been developed and the ideal model has been modified to take this effect into account. It has been used to describe the anti-Langmuirian peaks developing in non-adsorbing conditions. The porosity model parameters have been determined by fitting of the model to the experimental data and they were compared to the effect of salts on the peptide porosity. The modifier adsorption isotherm has been determined on all column studied and the correlation between the accumulation of modifier in the pores and the limited pore accessibility of the peptide has been shown.

2. Experimental

The experiments were carried out on a HP 1090 liquid chromatograph equipped with an auto-sampler, a diode array detector, an online-degasser (HP 1100 series) and a binary pump (HP 1100 series). HPLC grade acetonitrile was purchased from Sigma–Aldrich (Buchs, Switzerland). Calcium chloride, Sodium sulfate and *ortho*-phosphoric acid 85% were purchased from Merck (Darmstadt, Germany) and the sodium chloride from Mallinckrodt Baker (Deventer, Holland). All the chemicals were used without further purification. The deionized water was purified with a Simpak2 unit (Millipore, MA, USA) before use. Six different columns were used in this work. Among those six columns, three fully endcapped C18 silica based stationary phase and three polymeric phases were selected. The column characteristics given by the manufacturer are shown in Table 1. The peptide used in this work is a generic polypeptide with a molecular weight in the order of 3–4 kDa. The chemicals and experimental conditions are described in Table 2. All experiments were performed at pH 2.2 and at a flow rate of 1 mL/min. In those conditions, the peptide is protonated and carries a net positive charge.

Table 1
Characteristics of the columns used in this work. All values given above are provided by the manufacturer.

	Kromasil 100A, 10 u, C18	Eclipse XDB-C18	Daisogel SP-120-10-ODS-BP	Amersham Resource RPC, 3 mL	PLRP-S 300A, 10 u	PLRP-S 100A, 10 u
Stationary phase	Silica particle with C18 bonded chains	Silica particle with C18 bonded chains	Silica particle with C18 bonded chains	Polystyrene-divinylbenzene particle	Polystyrene-divinylbenzene particle	Polystyrene-divinylbenzene particle
Internal diameter (cm)	0.64	0.46	0.46	0.64	0.46	0.46
Length (cm)	25	15	25	10	25	15
Surface area (m^2/g)	330	180	300	–	384	414
Packed density (g/mL)	0.66	–	–	–	0.33	0.33
Particle size (μm)	10	5	10	15	10	10
Pore diameter (Å)	110	80	120	-	300	100

Table 2
Experimental conditions.

Type of measurement	Mobile phase composition
Peptide effect on its porosity	20 mM H_3PO_4, 58% (v/v) of acetonitrile
Salt effect on peptide porosity	20 mM H_3PO_4, 58% (v/v) of acetonitrile, various salts
Acetonitrile adsorption isotherm	20 mM H_3PO_4, acetonitrile

3. Peptide porosity as a function of its concentration

Increasing amounts of peptide were injected on various columns at high acetonitrile concentration (i.e. non-adsorbing conditions). The obtained elution profiles on the PLRP-S 100A column are shown in Fig. 2. Anti-Langmuirian peaks develop in these conditions, because the peptide porosity increases as the peptide concentration increases [16–18]. This phenomenon is due to electrostatic repulsion between the analyte and the positive charges present on the stationary phase [16,26–30]. The shielding of the analyte charges by other analytes present in the surrounding reduces in fact the electrostatic repulsion between the analyte and the stationary phase, by increasing locally the ionic strength. Therefore the analyte can come closer to the stationary phase surface and its pore accessibility increases.

This hypothesis has been tested by modifying the ideal model of a chromatographic column by introducing a porosity value which changes as a function of the analyte concentration. The corresponding mass balance on a slice of column can be expressed by:

$$(u_{sf}cS)_{z,t} - (u_{sf}cS)_{z+\Delta z,t} = \left\{ \frac{d}{dt}(c\varepsilon^*(c)S\Delta z + q(1-\varepsilon^*(c))S\Delta z) \right\}_{\bar{z},t} \quad (1)$$

c and q are the analyte concentrations, respectively, in the mobile and in the stationary phase, u_{sf} is the superficial velocity of the mobile phase, S is the section area of the column, $\varepsilon^*(c)$ is the column porosity, t is the time and Δz is the length of the slice. If an infinitely small slice is taken, the previous equation becomes a partial differential equation:

$$-u_{sf}\frac{\partial c}{\partial z} = \frac{\partial c}{\partial t}\left[\varepsilon^*(c) + (c-q)\frac{\partial \varepsilon^*(c)}{\partial c} + (1-\varepsilon^*(c))\frac{\partial q}{\partial c}\right] \quad (2)$$

In non-adsorbing condition, the analyte concentration in the stationary phase is equal to zero and the previous equation can be reduced as follows:

$$u_{sf}\frac{\partial c}{\partial z} + \frac{\partial c}{\partial t}\left[\varepsilon^*(c) + c\frac{\partial \varepsilon^*(c)}{\partial c}\right] = 0 \quad (3)$$

Using the dimensionless time $\tau_R = t_R u_{sf}/L$ and length $x = z/L$, with t_R being the retention time of the analyte and L the length of the column, we obtain:

$$\frac{\partial c}{\partial x} + \frac{\partial c}{\partial \tau}\left[\varepsilon^*(c) + c\frac{\partial \varepsilon^*(c)}{\partial c}\right] = 0 \quad (4)$$

This equation can be solved analytically using the method of characteristics [34]. The obtained solution representing the retention time of the analyte as a function of its concentration is given by:

$$\tau_R = \varepsilon^*(c) + c\frac{\partial \varepsilon^*(c)}{\partial c} \quad (5)$$

The porosity function used to fit the data is an empirical saturation-type function, which has been chosen for reasons indicated later. The porosity is assumed to vary from ε^*_{min} to ε^*_{max} depending on the analyte concentration:

$$\varepsilon^*(c) = \varepsilon^*_{min} + \frac{ac}{1 + \frac{a}{\varepsilon^*_{max} - \varepsilon^*_{min}}c} \quad (6)$$

The initial slope of the porosity variation is a. The minimal porosity experienced by the analyte is ε^*_{min}, which corresponds to the situation where the analyte concentration approaches zero. The porosity can increase up to a saturation value ε^*_{max} when the analyte concentration is sufficiently high. The boundaries of this function are justified since the analyte porosity cannot be smaller than the external porosity ($\varepsilon^*_{min} \geq \varepsilon_e$) and the maximum porosity is limited by the maximum liquid phase volume ideally available for an analyte of a certain size.

The chromatographic model developed above was used to fit the wave region of the anti-Langmuirian peaks. The dispersed front of the peaks shown in Fig. 2 was fitted with Eq. (5) assuming that the peptide porosity dependency can be described by Eq. (6). The experimental results and the fitted curve are in good agreement except on the top and the bottom of the peak (e.g. Fig. 3). These deviations are due to dispersion effects which are neglected in the model developed. The dispersed tails in Fig. 2 are due to extra-column effects, since the tailing is also observed for injections in the HPLC where the column has been removed (Fig. 4). Accordingly, this portion of the peak is not utilized in the rest of this work.

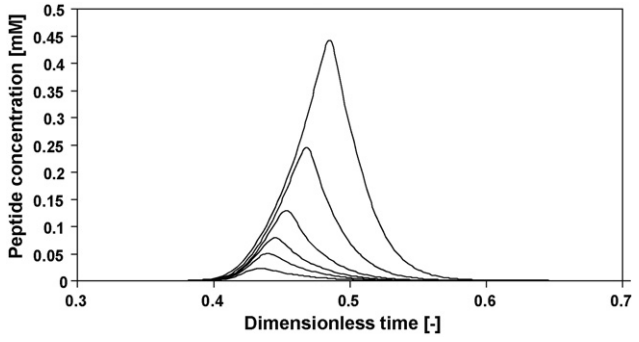

Fig. 2. Elution profiles of the peptide on PLRP-S 100A column in non-adsorbing conditions for increasing amounts of peptide. Injection of 1, 2, 3 5, 10, 20 μL of a 2.85 mM solution.

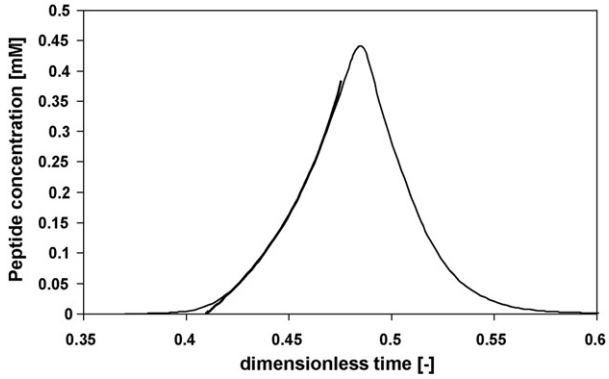

Fig. 3. Thin line: experimental elution profile of the peptide on PLRP-S 100A column. Injection of 20 μL of a 2.85 mM solution. Thick line: fitting of Eq. (5) to the dispersed front.

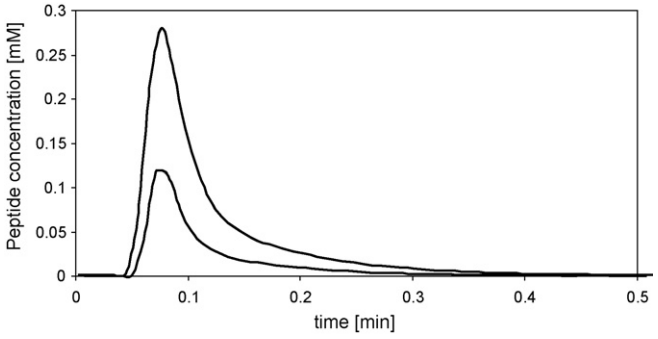

Fig. 4. Elution profiles of the peptide without a column connected to the HPLC. Injection of 3 and 10 μL of a 2.85 mM solution.

The estimated parameters of Eq. (6) for all columns after fitting are summarized in Table 3. It is seen that ε^*_{min} is equivalent to typical values for the external porosity of packed column (i.e. 0.37–0.4) on columns having small pore size (dp = 100 Å) such as the PLRP-S 100A and the Daisogel C18. In this case, the peptide is totally excluded from the pores when a low amount of peptide is injected. For columns having larger pore sizes (e.g. RPC and PLRP-S 300A), ε^*_{min} tends to take larger values indicating that in this case, the peptide can enter the pores to a certain extent even at low peptide concentration. In the case of the Kromasil C18 and the Eclipse XDB, the peptide is pore excluded as in the case of the PLRP-S 100A and the Daisogel C18, but the anti-Langmuirian peaks do not develop in non-adsorbing conditions (Fig. 5). It will be shown in the next section that an effect of the ionic strength on the porosity is observed on those columns, but only to a very limited extent and that the porosity variation induced by the peptide concentration is therefore too weak for the development of anti-Langmuirian peaks in non-adsorbing conditions, this phenomenon being hidden by the dispersion effects. Moreover, the low peptide pore accessibility observed on those columns, even in a high ionic strength environment, will be justified by the large accumulation of acetonitrile in the pores as it will be explained in more details in Section 5.

Table 3
Fitted parameters of Eq. (6).

	a (L/mol)	ε^*_{min}	ε^*_{max}
RPC	185.32	0.61	0.71
PLRP-S 300A	180.44	0.53	0.62
PLRP-S 100A	178.68	0.41	0.51
Daisogel C18	73.70	0.40	0.50

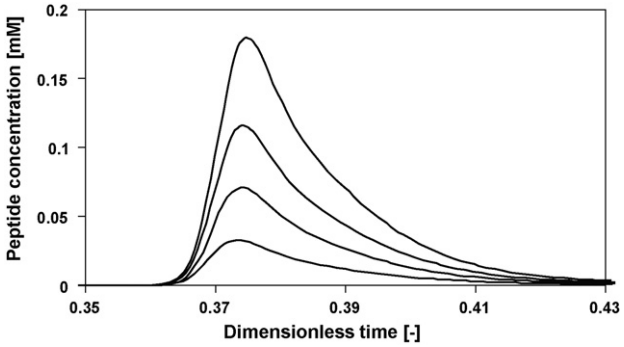

Fig. 5. Elution profiles of the peptide on the Kromasil C18 column for increasing value of the peptide concentration. Injection of 1, 2, 3, 5 μL of a 2.85 mM solution.

4. Peptide porosity as a function of salt concentration

In the previous section, we showed that anti-Langmuirian peaks develop when the peptide is injected into the column in non-adsorbing conditions. If this phenomenon is due to electrostatic effects as proposed by Berendsen et al. [16], the effect of salt on the porosity has to be the same as the one of the peptide, since the peptide charges can be shielded by both species. The peptide porosity as a function of salt concentration was determined and compared to the porosity variation induced by the peptide concentration.

The retention times of small peptide injections were measured in non-adsorbing conditions at various salt concentrations in the eluent. The peptide porosity was then calculated from the retention time. The results obtained on the RPC column are shown in Fig. 6. The increase of the peptide porosity as a function of salt concentration follows the same behavior as the peptide porosity variation induced by the peptide concentration itself. The apparent differences between the salts vanish when the porosity variation is described as a function of the concentration of negative charges, as it can be seen in Fig. 7. This shows that the screening of the peptide charges is a function of the concentration of negative charges in the eluent and not a function of the concentration of salt. In fact, the peptide is positively charged at low pH (i.e. in the working conditions) and the screening of the peptide charges is carried out by the negative charges only. It can be therefore seen that all salts have the same effect on the peptide porosity, this effect being described by an equation similar to Eq. (6):

$$\varepsilon^*(c_{charges}) = \varepsilon^*_{min} + \frac{a c_{charges}}{1 + \frac{a}{\varepsilon^*_{max} - \varepsilon^*_{min}} c_{charges}} \quad (7)$$

The porosity boundaries ε^*_{min} and ε^*_{max} determined in this case turn out to be the same as the ones determined for the porosity variation due to the peptide concentration (Table 4). This is consistent with the fact that the porosity variation induced by the peptide

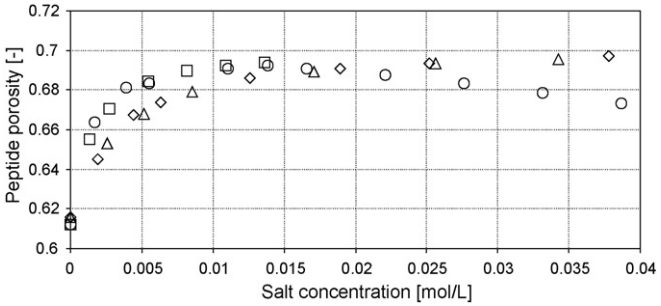

Fig. 6. Peptide porosity as a function of the salt concentration in the eluent on the RPC 3 mL column. Squares: $CaCl_2$, triangles: NaCl, circles: Na_2SO_4, and diamonds: NaBr.

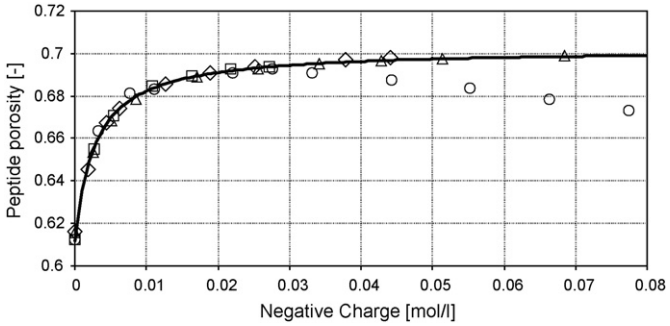

Fig. 7. Peptide porosity as a function of the concentration of negative charges in the eluent on the RPC 3 mL column. Squares: $CaCl_2$, triangles: NaCl, circles: Na_2SO_4, diamonds: NaBr, line: fitting of Eq. (7) with $a = 32.4$ L/mol, $\varepsilon_{min} = 0.61$, $\varepsilon_{max} = 0.70$.

Table 4
Fitted parameters of Eqs. (6) and (7) for the RPC 3 mL column.

	a (L/mol)	ε^*_{min}	ε^*_{max}
Salt	32.42	0.61	0.70
Peptide	185.32	0.61	0.71

concentration is due to the same phenomenon as the porosity variation induced by the salt concentration in the eluent. Eq. (6) can be thus seen as a special case of Eq. (7), when the peptide charges are screened by its own charges.

In Figs. 6 and 7, it is seen that, in the case of sodium sulfate, the peptide porosity reaches a maximum and then decreases when the salt concentration is further increased. We believe that this is due to a complex formation involving two peptides and a sulfate ion. The peptide porosity decreases with the formation of this complex, because the apparent increase of the peptide size reduces its pore accessibility. The formation of analyte complexes in the presence of divalent ions has been already observed by Gritti and Guiochon [35]. They have shown that this phenomenon increases adsorbate–adsorbate interactions, thus leading to anti-Langmuirian behavior in adsorbing conditions. The effect of divalent ions on the peptide behavior in both adsorbing and non-adsorbing conditions needs, however, further studies.

A similar behavior as those described above is found for all columns studied in this work, although the porosity changes are much less pronounced in the case of the Eclipse XDB and the Kromasil C18 columns (e.g. Fig. 8). It shows that electrostatic repulsions between the peptide and the stationary phases are present in all type of columns considered in this work (i.e. silica based C18 and polymeric stationary phases), although the porosity variation might be too weak for the development of anti-Langmuirian peaks as described in the previous section. The similar behavior observed on silica based and polymeric stationary phases allows us to conclude

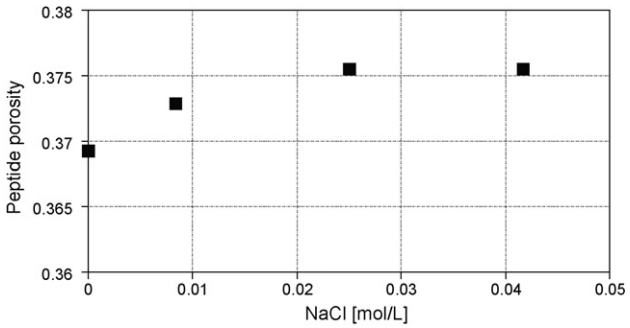

Fig. 8. Peptide porosity as a function of the sodium chloride concentration in the eluent on the Kromasil C18 column.

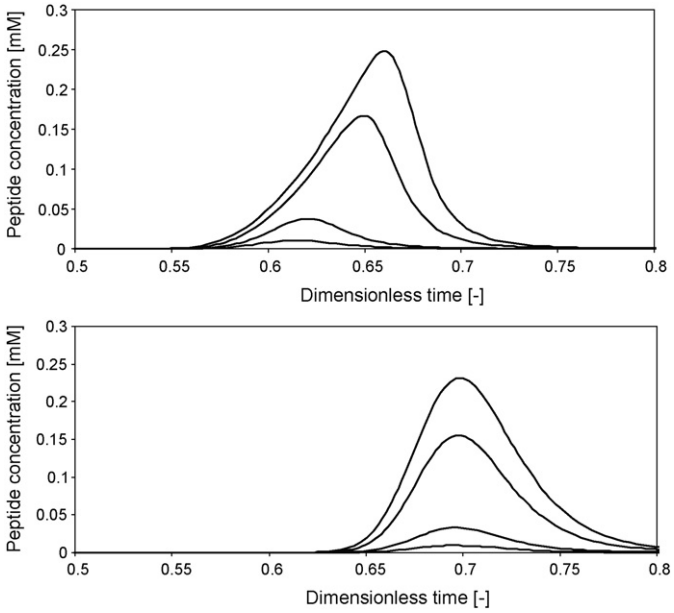

Fig. 9. Elution profile of the peptide on the RPC 3 mL column for increasing values of the peptide concentration. (a) No salts, (b) 1 g/L sodium chloride in the eluent. Injection of 3, 10, 50, 80 μL of a 2.85 mM solution.

that the presence of positive charges on the stationary phase is not due to the chemical nature of the hydrophobic surface, but comes from a general tendency of hydrophobic surfaces at low pH. The preferential adsorption of cations relative to anions as suggested by Okada [27] could be a possible explanation.

Let us now examine the effect of the peptide concentration on the porosity in an eluent containing salt. The elution profiles of the peptide on the RPC 3 mL column in an eluent containing sodium chloride or not are compared in Fig. 9a and b, respectively. As discussed above, without salt in the eluent, the anti-Langmuirian peaks appear since the increase of the ionic strength due to the peptide concentration leads to an increase of the peptide porosity (Fig. 9a). With 17 mM of sodium chloride in the eluent, the peaks are Gaussian (i.e. constant porosity), since the porosity experienced by the peptide is already maximal when a small pulse of peptide is injected (Fig. 9b). The further increase of the ionic strength by the peptide does not affect the porosity, the latter remaining equals to ε^*_{max}, since all the peptide charges are already screened by the presence of the salt in the eluent. This finding confirms that the anti-Langmuirian peak shapes observed in non-adsorbing conditions are due to a porosity variation induced by the local amount of negative charges.

5. Effect of the modifier adsorption on the peptide porosity

The results reported above indicate that the particle porosity accessible to the peptide (ε_p) in non-adsorbing conditions is very small (Table 5). This is true in particular for the Kromasil C18 and the Eclipse XDB where ε_p does not exceed 0.1 even in a high ionic

Table 5
Particle porosity accessible to the peptide.

Column	$\varepsilon^*_{p,min}$	$\varepsilon^*_{p,max}$
Daisogel C18	0.05	0.21
PLRP-S 100A	0.06	0.23
PLRP-S 300A	0.25	0.39
RPC	0.38	0.56
Kromasil C18	0.00	0.01
Eclipse XDB	0.07	0.08

strength eluent. On the other hand, under adsorbing conditions (i.e. when the acetonitrile concentration is strongly reduced), it is known that significant loading of the peptide can be achieved, which is clearly not compatible with the low porosity values measured under non-adsorbing conditions. In this section we show that this behavior can be explained by the accumulation of acetonitrile in the pore volume which hinders significantly the pore accessibility of the peptide in non-adsorbing conditions.

5.1. Acetonitrile adsorption isotherm determination

The adsorption of the modifier can in fact be regarded as an accumulation in a close proximity to the solid phase surface and it can be represented by an excess adsorption isotherm following Kazakevich [36]. The method used for the acetonitrile adsorption isotherm determination is the minor disturbance method [7,11,33,37,38]. The retention volumes (V_R) of small perturbations at different plateau of acetonitrile concentration c_{AcN} are measured and are numerically integrated using Eq. (8) to give the excess adsorption isotherm $\Gamma_{AcN}(c_{AcN})$:

$$\Gamma_{AcN}(c_{AcN}) = \frac{1}{S}\int_0^{c_{AcN}} (V_R(c_{AcN}) - V_0)\mathrm{d}c_{AcN} \quad (8)$$

where S is the surface available for adsorption and V_0 is the total liquid volume in the column and is determined from the integration of the retention volumes over the entire range of concentration:

$$V_0 = \frac{\int_0^{c_{AcN,max}} V_R(c_{AcN})\mathrm{d}c_{AcN}}{c_{AcN,max}} \quad (9)$$

The obtained values are represented by the squares in Fig. 10. Using the method proposed by Everett [39], the maximum amount adsorbed is determined by back-extrapolation of the excess adsorption isotherm in the linear region (50–80% AcN in Fig. 10) to the intercept with the y-axis (thin line in Fig. 10). This corresponds to the amount adsorbed when the mobile phase is composed of pure acetonitrile. The straight line between the origin and the amount adsorbed in pure acetonitrile represents the equilibrium concentration (thick line in Fig. 10). By addition of the excess adsorbed to the equilibrium concentration, the adsorption isotherm $q_{AcN}(c_{AcN})$ is obtained:

$$q_{AcN}(c_{AcN}) = \frac{c_{AcN} \times V_a(c_{AcN})}{S} + \Gamma(c_{AcN}) \quad (10)$$

The acetonitrile adsorption isotherm was measured on several columns. The obtained results are shown in Figs. 11 and 12. Note that the adsorption isotherms in Figs. 11 and 12 are referred to the solid phase volume $V_s = V_C - V_0$ instead than to the solid phase

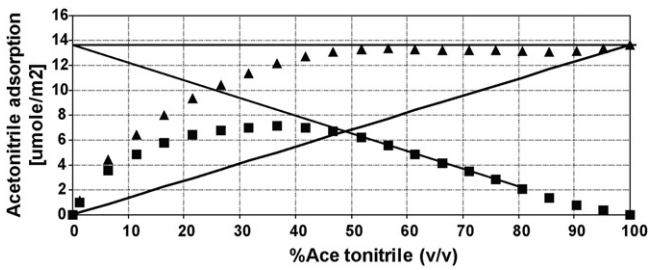

Fig. 10. Determination of the adsorption isotherm of acetonitrile on the PLRP-S 300A column. Squares: excess adsorption isotherm. Thick line: equilibrium concentration. Triangles: adsorption isotherm.

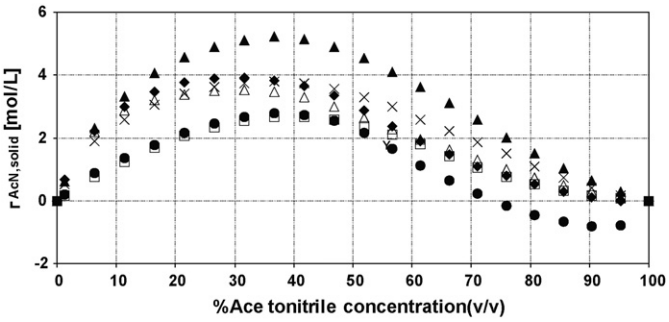

Fig. 11. Excess adsorption isotherm of acetonitrile. Squares: Kromasil C18 column. Empty triangles: Eclipse XDB column. Filled triangles: PLRP-S 100A column. Diamonds: Amersham RPC 3 mL column. Crosses: PLRP-S 300A column. Circles: Daisogel C18 column. Stars: Daisogel C8 column.

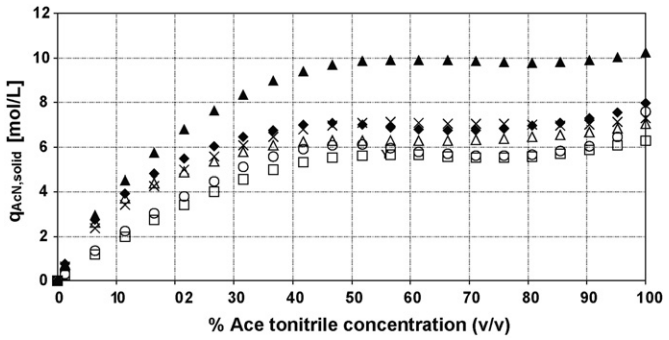

Fig. 12. Adsorption isotherm of acetonitrile. Squares: Kromasil C18 column. Empty triangles: Eclipse XDB column. Filled triangles: PLRP-S 100A column. Diamonds: Amersham RPC 3 mL column. Crosses: PLRP-S 300A column. Circles: Daisogel C18 column.

$$\text{surface: } \Gamma_{AcN,solid}(c_{AcN}) = \frac{1}{V_S}\int_0^{c_{AcN}} (V_R(c_{AcN}) - V_0)dc_{AcN}$$

$$\Gamma_{AcN,solid}(c_{AcN}) = \frac{1}{V_S}\int_0^{c_{AcN}} (V_R(c_{AcN}) - V_0)\mathrm{d}c_{AcN} \quad (11)$$

$$q_{AcN,solid}(c_{AcN}) = \frac{c_{AcN} \times V_a(c_{AcN})}{V_S} + \Gamma_{AcN,solid}(c_{AcN}) \quad (12)$$

From the adsorption isotherm, it is possible to determine the thickness of the adsorbed layer $\tau(c_{AcN})$ by introducing the concept of dividing plane [31] which assumes that the adsorbed phase is composed of pure acetonitrile:

$$\tau(c_{AcN}) = \frac{V_a(c_{AcN})}{S} \quad (13)$$

The surface area used in the calculation of the adsorbed layer thickness is taken from nitrogen adsorption data supplied by the manufacturer. The acetonitrile adsorbed phase thickness measured is reported in Table 6 and is comparable to the ones found in the literature for usual reversed-phase column [31] (last row in Table 6). It indicates that acetonitrile forms a multi-layer adsorbed phase.

Table 6
Thickness of the acetonitrile adsorbed layer calculated from the adsorption isotherm of acetonitrile. Data for C1 to C18 monomeric phases taken from [34].

	Thickness (Å)
Kromasil C18	6.3
PLRP-S 300A	7.2
PLRP-S 100A	10.7
C1–C18 monomeric phases	10–15

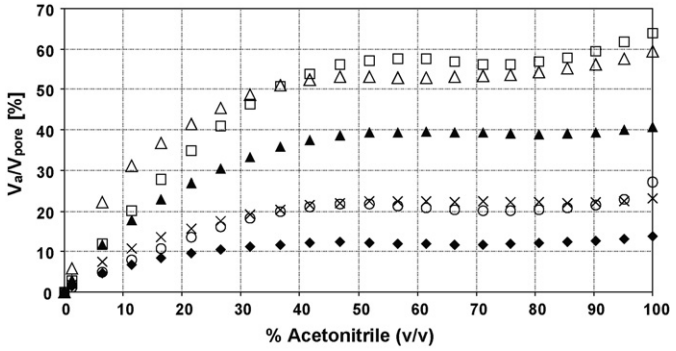

Fig. 13. Percentage of the pore volume filled with acetonitrile as a function of the acetonitrile concentration in the eluent. Squares: Kromasil C18 column. Empty triangles: Eclipse XDB column. Filled triangles: PLRP-S 100A column. Diamonds: Amersham RPC 3 mL column. Crosses: PLRP-S 300A column. Circles: Daisogel C18 column.

5.2. Effect of the acetonitrile adsorption on the peptide porosity

As stated earlier the accumulation of acetonitrile in the pores has an impact on the peptide porosity. The peptide porosity decreases when the acetonitrile concentration is increased. At high acetonitrile concentration, the peptide can be almost completely excluded from the pores due to the acetonitrile accumulation as it is the case for the Kromasil C18 and the Eclipse XDB columns. To highlight this effect, the percentage of the pore volume filled with acetonitrile is calculated:

$$V_{\mathrm{AcN/pore}} = \frac{V_a(c_{\mathrm{AcN}})}{V_{\mathrm{pore}}} \times 100 = \frac{V_a(c_{\mathrm{AcN}})}{V_0 - V_e} \times 100 \qquad (14)$$

where V_{pore} is the total volume of the pores. $V_a(C_{\mathrm{AcN}})$ is the volume of acetonitrile. V_0 is the total liquid phase volume as determined from minor disturbance measurements (Eq. (9)) and V_e is the interstitial liquid volume.

The percentage of the pore volume filled with acetonitrile for the six columns considered in this work is shown in Fig. 13. It can be observed that the percentage of the pore volume filled with acetonitrile decreases with the pore size. In fact the PLRP-S 100A has more acetonitrile accumulated in the pores than the PLRP-S 300A. This can be justified by the larger surface/volume ratio in columns having small pores. The differences among the columns having similar pore sizes is, however, difficult to explain due to the differences in pore size distribution and in the chemical nature of the stationary phases.

The Kromasil C18 column and the Eclipse XDB column have a higher amount of acetonitrile accumulated in the pores compared to the other columns. The acetonitrile adsorbed layer on those columns fills more than 45% of the pore volume at high acetonitrile concentration and limits therefore the access of the peptide to the pores. The effect of the ionic strength on the peptide porosity is weak on these columns (e.g. Fig. 8), since the acetonitrile adsorbed layer limits strongly the maximal volume accessible for the peptide (i.e. volume accessible in a high ionic strength environment). The peptide can efficiently enter the pores in adsorbing condition (i.e. low acetonitrile concentration), since the adsorbed phase is thinner in this case, justifying therefore the high loading possible onto these columns. The peptide porosity is thus a function of the acetonitrile adsorbed. On the other columns there is less accumulation of acetonitrile in the pores, the peptide is therefore less excluded from the pores in non-adsorbing conditions. The effect of the ionic strength on the pore availability is therefore stronger as it was shown in previous sections.

6. Conclusions

The peptide pore accessibility has been studied for six different stationary phases. It has been shown that, the peptide porosity depends upon the peptide and salt concentration. The accessible porosity is, in fact, found to increase with the local concentration of negative charges following a saturation-type function within the same porosity boundaries for both cases. In a low ionic strength eluent, the peptide is partially or totally pore excluded in non-adsorbing conditions depending upon the stationary phase considered. When the ionic strength is increased by addition of salt in the eluent or by increasing the amount of peptide injected, the pores become accessible to the peptide. In the case of the porosity variation induced by the amount of peptide injected, anti-Langmuirian peaks are formed since the local ionic strength is affected by the peptide concentration and therefore the accessibility of the stationary phase increases with the peptide concentration. It has been also shown that the accumulation of acetonitrile in the pores affect the pore accessibility of the peptide. In fact, by measurement and comparison of the acetonitrile isotherm on all the stationary phases considered, it has been shown that the peptide is totally pore excluded when the stationary phases have more than 45% of the pore volume filled by acetonitrile.

The differences in the porosity measured at various experimental conditions can be explained by pore hindering induced by the acetonitrile accumulation and by the electrostatic interactions present between the peptide and the stationary phase. It is very important to account for these effects when modeling chromatographic processes. For example, in the case of peptide purification, the different molecules (including the modifier) may experience different porosities and this affects their degree of competition along the column and in general their chromatographic behavior. Another important aspect is the adsorption isotherm evaluation. In order to correctly evaluate the Henry coefficients from retention time measurements, the proper porosity has to be determined (i.e. the porosity experienced by the analyte in the actual experimental conditions), which is usually a quantity that can not be directly measured, but that can be computed from porosity variation models.

References

[1] L. Aumann, A. Butte, M. Morbidelli, K. Buscher, B. Schenkel, Sep. Sci. Technol. 43 (2008) 1310.
[2] J. Mohammad, B. Jäderlund, H. Lindblom, J. Chromatogr. A 852 (1999) 255.
[3] S. Linde, B.S. Welinder, J. Chromatogr. 548 (1991) 195.
[4] B.S. Welinder, J. Chromatogr. 542 (1991) 83.
[5] B.S. Welinder, H.H. Sorensen, J. Chromatogr. 537 (1991) 181.
[6] B. Trathnigg, M. Veronik, A. Gorbunov, J. Chromtogr. A 1104 (2006) 238.
[7] R.M. McCormick, B.L. Karger, Anal. Chem. 52 (1980) 2249.
[8] E.H. Slatts, W. Markovski, J. Fekete, H. Poppe, J. Chromatogr. 207 (1981) 299.
[9] C.R. Yonker, T.A. Zwier, M.F. Burke, J. Chromatogr. 241 (1982) 257.
[10] N.L. Ha, J. Ungvaral, E. sz Kovats, Anal. Chem. 54 (1982) 2410.
[11] Y.V. Kazakevich, H.M. McNair, J. Chromatogr. Sci. 31 (1993) 317.
[12] K.S. Yun, C. Zhu, J.F. Parcher, Anal. Chem. 67 (1995) 613.
[13] C.A. Rimmer, C.R. Simmons, J.G. Dorsey, J. Chromatogr. A 965 (2002) 219.
[14] W. Piatkowski, F. Gritti, K. Kaczmarski, G. Guiochon, J. Chromatogr. A 989 (2003) 207.
[15] F. Gritti, G. Guiochon, J. Chromatogr. A 1176 (2007) 107.
[16] G.E. Berendsen, P.J. Schoenmakers, L. de Galan, G. Vigh, Z. Varga-Puchony, J. Inczedy, Liq. J. Chromatogr. 3 (1980) 1669.
[17] M.J.M. Wells, C.R. Clark, Anal. Chem. 53 (1981) 1341.
[18] F.A. Buytenhuys, F.P.B. Van Der Maeden, J. Chromatogr. 149 (1978) 489.
[19] F. Gritti, G. Guiochon, Anal. Chem. 76 (2004) 4779.
[20] F. Gritti, G. Guiochon, J. Chromatogr. A 1033 (2004) 57.
[21] F. Gritti, G. Guiochon, J. Chromatogr. A 1033 (2004) 43.
[22] F. Gritti, G. Guiochon, J. Chromatogr. A 1047 (2004) 33.
[23] T.J. Sereda, C.T. Mant, R.S. Hodges, J. Chromatogr. A 776 (1997) 153.
[24] P.A. Neddermeyer, L.B. Rogers, Anal. Chem. 41 (1969) 94.
[25] M.P. Tsyurupa, V.A. Danakov, Doklady Chem. 398 (2004) 184.
[26] E. Loeser, J. Chromatogr. Sci. 46 (2008) 45.
[27] T. Okada, Anal. Chem. 72 (2000) 1307.
[28] A. Méndez, E. Bosch, M. Rosés, U.D. Neue, J. Chromatogr. A 986 (2003) 33.

[29] D.V. McCalley, J. Sep. Sci. 26 (2003) 187.
[30] E. Loeser, P. Drumm, Anal. Chem. 79 (2007) 5382.
[31] Y.V. Kazakevich, R. LoBrutto, F. Chan, T. Patel, J. Chromatogr. A 913 (2001) 75.
[32] N.L. Ha, J. Ungvaral, E. Kovats, Anal. Chem. 54 (1982) 2410.
[33] F. Chan, L.S. Yeug, R. LoBrutto, Y.V. Kazakevich, J. Chromatogr. A 1082 (2005) 158.
[34] R. Hyun-Ku, A. Rutherford, N.R. Amundson, First-Order Partial Differential Equations, vol. 1, Dover Publications, 2001.
[35] F. Gritti, G. Guiochon, J. Chromatogr. A 1038 (2004) 53.
[36] Y.V. Kazakevich, J. Chromatogr. A 1126 (2006) 232.
[37] J. Knox, R. Kaliszan, J. Chromatogr. 349 (1985) 211.
[38] Y.A. Eltekov, Y.V. Kazakevich, J. Chromatogr. 395 (1987) 473.
[39] D.H. Everett, J. Chem. Soc. Faraday Trans. I 60 (1964) 1803.